

Long Distance Photoinduced Electron Transfer in Solutions: A Mechanism for Producing Large Yields of Free Ions by Electron Transfer Quenching

Jinwei Zhou,* Roshan P. Shah, Bret R. Findley, and Charles L. Braun*

Department of Chemistry, 6128 Burke Laboratory, Dartmouth College, Hanover, New Hampshire 03755

Received: July 23, 2001; In Final Form: October 29, 2001

Free ion and fluorescence quantum yields from the geminate ion pairs formed by electron-transfer quenching of the excited acceptor 9,10-dicyanoanthracene by aromatic electron-donors are measured in different solvents. The effects of solvent polarity, energetic driving force, and steric substitution on free ion yields are studied. From the comparison of the effect of driving force on free ion yields and fluorescence quantum yields in different solvents, especially those of moderate polarity, it is concluded that free ion yields are controlled by both recombination rate constants and the separation distance distribution of the initially formed geminate radical ion pairs. In dichloromethane (DCM), the recombination and free ion formation processes are directly observed by fluorescence lifetime and transient photocurrent measurements. The time-resolved results indicate that free ion formation is faster than the recombination process. This means that the geminate radical ion pairs that form free ions and those that are neutralized by electron-transfer recombination have different histories with different separation distances. From studies of steric effects on free ion yields in different solvents, it is concluded that, in polar solvents such as acetonitrile and butyronitrile, the main effect of steric hindrance is to decrease the recombination rate constant and increase the escape probability, whereas in moderately polar solvents such as tetrahydrofuran, DCM and 1,2-dichlorobenzene, the main effect of steric bulk is to change the initial separation distance distribution of the geminate radical ion pairs formed by electron-transfer quenching. As an example, we compare donors such as durene (DUR) with those of greater steric bulk like 1,2,4,5-tetra-*iso*-propylbenzene (TIPB), for which the driving force for electron transfer is similar. The free radical ion yield for TIPB is more than 40 times greater than it is for DUR in DCM. This is the first example from our work in which the infinite rate boundary condition for ion recombination used by Onsager is not adequate, because there is no perfect sink at the origin. The free ion yield data are analyzed by the theory of Hong and Noolandi under the Collins and Kimball boundary condition.

1. Introduction

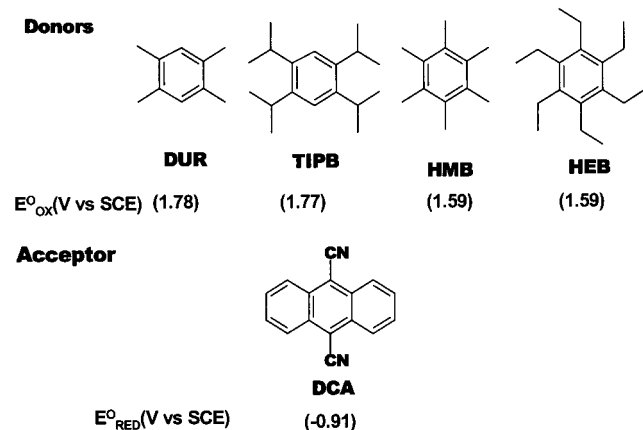
Photoinduced charge-transfer processes for electron donor–acceptor systems in solid state^{1,2} or bridge-linked molecules^{3–8} are relatively simple because the distance between the reactants is fixed. For photoinduced bimolecular donor-to-acceptor electron transfer in solutions, the processes are much more complex. In solution, steady-state and time-resolved measurements indicate that different intermediate species such as exciplexes,^{9,10} contact radical ion pairs (CRIPs),^{11–13} solvent-separated radical ion pairs (SSRIPs),^{12,13} loose radical ion pairs (LRIPs),¹⁴ or free radical ions (FRIs)^{11,15} can be formed after photoexcitation. Despite extensive study of the photophysics and chemistry of exciplexes and excited EDA complexes, the relative contributions of exciplexes, CRIPs, and LRIPs in charge separation, charge recombination, and free ion formation are still not clear.¹⁶ At the center of this problem is the initial separation distance distribution for geminate radical ion pairs and its effect on the subsequent charge recombination and FRI formation processes.

It has long been believed that direct photoexcitation of EDA complexes will result in the formation of contact radical ion pairs (CRIPs) with an initial charge separation distance of about 3.5 Å, which can either separate into LRIPs in polar solvents by solvation or recombine via electron transfer.^{13,17} Generally, this model works well for understanding the charge recombination process. However, in recent work, we found that when EDA

complexes are excited experimental free ion yields are much greater than those predicted for CRIPs by Onsager's escape probability equation,¹⁸ especially in low to medium polarity solvents. This discrepancy can be as large as several orders of magnitude (*vide infra*) and suggests that some large ion separation distances are also created upon excitation. In further work,¹⁹ we measured the free radical ion (FRI) quantum yields of several EDA systems composed of alkylbenzene electron donors with the electron acceptor tetracyanoethylene (TCNE) in dichloromethane. It was found that absorption in or near a charge transfer (CT) band is due to both EDA complexes and unassociated donor–acceptor (D...A) random pairs and that FRI yields for these systems exhibit a strong dependence on both the excitation wavelength and the equilibrium constant of D/A association. The radical ion pairs (RIPs) resulting from the excitation of long-distance random pairs make the predominant contribution to the FRI yield. Although this long distance photoinduced electron transfer may not significantly affect charge recombination, it is crucial to charge separation. To address quantitatively the relationship between initial separation distance distribution and free ion yields, we developed a model to calculate the contribution of distant (D...A) pairs to the FRI quantum yields and compared our predictions with experimental results at each excitation wavelength.²⁰ In our model, Mulliken–Hush expressions were used for absorption in the CT band and the Onsager equation was used to calculate the escape probability.

* To whom correspondence should be addressed.

SCHEME 1



For geminate ion pairs formed by quenching,⁹ it has long been noted that the intensity of exciplex fluorescence decreases much faster than the lifetime when the solvent dielectric constant increases. This is interpreted to mean both that the exciplex decays more quickly in polar solvents than in nonpolar solvents and that the probability of exciplex formation is lower in polar solvents than in nonpolar solvents. There are two different kinds of quenching reactions. The first gives the fluorescent exciplex, the lifetime of which declines with increasing dielectric constant because of increased dissociation into free ions. The competing second reaction is supposed to produce a solvent-separated nonfluorescent ion pair that dissociates with high probability. Given that the free ion yield is more sensitive than recombination to the change in initial ion separation distance, it is of interest to expand our free ion yield experiment to quenching systems.

Free ion formation and recombination processes are also sensitive to changes in solvent polarity. Thus far, most of the photoinduced electron-transfer reactions in solution have been made in polar solvents such as acetonitrile,^{11,13,16,21–24} in which the geminate ion pairs formed have a high probability of solvation and separation, giving a large free ion yield. The disadvantage of using a strongly polar solvent is that the energy difference is small among radical ion pairs of different separation distances. This makes the free ion yield insensitive to changes in the initial separation for highly polar solvents. In this work, solvents of different polarities and donors with different steric bulk are used, which allows the probing of the effects of both driving force and separation distance distribution on free ion yields.

2. Experimental Section

9,10-Dicyanoanthracene (DCA) from Aldrich was used as the acceptor in this work. Donors used were durene (DUR; Aldrich, 98%), 1,2,4,5-tetraisopropylbenzene (TIPB; Aldrich, 96%), hexamethylbenzene (HMB; Aldrich, 99%), and hexaethylbenzene (HEB, Aldrich). Solvents used were acetonitrile (AN; Fisher, 99%), butyronitrile (BN; Aldrich, 99%), dichloromethane (DCM; Fisher, 99%), 1,2-dichlorobenzene (DCB; Acros, 99%), and tetrahydrofuran (THF; Aldrich, 99%). The structures, oxidation (E_{OX}^0) or reduction (E_{RED}^0) potentials²¹ of the donors, and acceptors used are given in Scheme 1.

In transient photocurrent experiments, excitation of the sample solution was performed using third harmonic generation (355 nm) from a MPB Technologies Orion SB-R Nd:YAG laser with a full width at half-maximum (fwhm) of 0.4 ns. Pulse energies were between 20 and 35 μJ within a 0.015 cm^2 spot size. A

continuous-flow “fast” cell, consisting of two parallel stainless steel electrodes separated by 0.96 mm, with 1.0 cm optical path length was used in the present study. A steady state voltage is applied by the HV power supply across the electrode gap of the cell. The applied voltages are from 400 to 1600 V, and in most cases, the experiments are performed at 400 to 800 V. The experiment was conducted in the charge displacement mode using an impedance probe as the load resistor R (varied from 50 Ω to 10 k Ω). Photoinduced currents were measured by a Tektronix TDS 684A oscilloscope. Model J4-09 Molelectron detectors were used to monitor incident and transmitted laser pulse energies. On the basis of repeated experiments, the internal error in free ion yield is about 4%. While the error in laser energy measurement using the J4-09 detector could be as large as 10%, this could result in a systematic error in the free ion yield measurement as large as 10%. A detailed description of the method used for photoinduced current measurements can be found in our previous work.^{18,19,25} All experiments were performed at room temperature (21 ± 1 °C). The absorbance of the solutions used in the photocurrent experiment was about 0.6 at 355 nm in a 1 cm cell. The solutions were deoxygenated by bubbling nitrogen. The concentrations of donors were 0.02–0.2 M. The free ion yields were normalized to 100% quenching efficiency.

Fluorescence spectra were recorded using a Perkin Elmer LS 50. Fluorescence lifetimes were measured using time correlated single photon counting. A 355 nm laser pulse from NV-20001-100 (Uniphase) was used for excitation. The pulses had a duration of 0.8 ns at 13 kHz and an average power of 1 mW. The emission was collected at 90° through a monochromator with a bandwidth of 3 nm located in front of the photomultiplier tube. The output from the single photon counting system was connected to a computer board module (Mca 32). For fluorescence experiments, the absorbance at 355 nm was about 0.1 in a cell with a 1 cm path length.

3. Results

At the donor concentrations used in the present study, no obvious EDA complex formation can be observed. Absorption and the fluorescence excitation spectra show similar shapes and are identical to solutions containing just DCA. Figure 1 shows the emission spectra of 1.0×10^{-5} M DCA in the absence and presence of different concentrations of DUR and TIPB. It is apparent from these spectra that DUR is a more effective quencher in DCM than is TIPB. For solutions containing DUR and DCA at high concentrations of DUR, a broad band appears around 520 nm. This is the characteristic exciplex emission^{9,10} and its intensity is ca. 8% of DCA monomer emission. For HMB-DCA, similar results can be observed, but the exciplex emission intensities are only about 1.4% of that for the monomer. The emission quantum yields from exciplexes of DCA-DUR and DCA-HMB in different solvents were determined and are collected in Table 2. The fluorescence lifetimes of DCA monomer in AN, BN, DCB, DCM, and THF were measured by single photon timing to be 12.1, 10.6, 11.2, 11.3, and 10.6 ns, respectively.

Electron-transfer quenching rate constants, k_q , are determined from Stern–Volmer plots and are also listed in Table 2. In polar solvents such as AN and BN, all four donors used in the present work are efficient quenchers of DCA. The second-order rate constants for fluorescence quenching are little affected by increased steric bulk of the donor. From DUR to the bulkier TIPB, k_q decreases ca. 50%. From HMB to HEB, k_q decreases only ca. 30%.

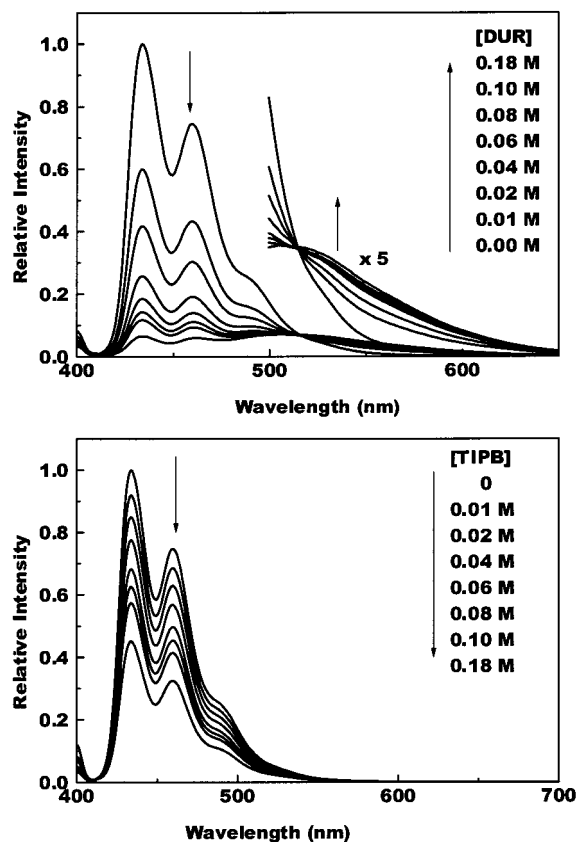


Figure 1. Emission spectra of 1.0×10^{-5} M DCA in DCM with different concentrations of DUR (a) or TIPB (b) after excitation at 355 nm.

TABLE 1: Abbreviations

AN	acetonitrile
BN	butyronitrile
CRIP	contact radical ion pair
CT	charge transfer
DCA	9,10-dicyanoanthracene
DCB	1,2-dichlorobenzene
DCM	dichloromethane
DUR	durene
EDA	electron-donor-acceptor
FRI	free radical ion
HEB	hexaethylbenzene
HMB	hexamethylbenzene
LRIP	loose radical ion pair
RIP	radical ion pair
SSRIP	solvent separated radical ion pair
THF	tetrahydrofuran
TIPB	1,2,4,5-tetra- <i>iso</i> -propylbenzene

When less polar solvents such as DCB, DCM, and THF are used, DUR is still an effective quencher, whereas TIPB is a relatively poor. The quenching rate constants, k_q , for TIPB in these solvents are reduced by more than 90% in comparison to those of DUR. The oxidation potentials for DUR and TIPB are the same. The only difference between the two that could affect their quenching ability is that DUR can get closer to DCA than can TIPB. The contact separation distance between TIPB and DCA is about 1.3 \AA^{26} larger than that for DUR and DCA. As shown in Table 2, k_q for DUR is more than 10 times greater than for TIPB. Assuming that long distance electron-transfer quenching for DUR and TIPB are the same, the difference in k_q values suggests that more than 90% of the quenching of DCA by DUR takes place at short separation distances between r_0 and $r_0 + 1.3 \text{ \AA}$. From HMB to HEB, the changes in oxidation potential and contact separation distance are similar to those from DUR to TIPB, but in most cases, the change in their

TABLE 2: Free Ion Yields (Y_{FRI}) for DUR, TIPB, HMB, and HEB with DCA in AN ($\epsilon = 37.5$), BN ($\epsilon = 24.9$), DCM ($\epsilon = 8.93$), DCB ($\epsilon = 9.93$), and THF ($\epsilon = 7.58$)

donor	solvent	k_q	Φ_F	Y_{FRI}^a
DUR	AN	1.5×10^{10}	0.0045 ^b	0.19 (0.239 ^c)
TIPB	AN	6.5×10^9		0.51 (0.549 ^d)
HMB	AN	1.7×10^{10}	0.0023 ^b	0.079 (0.078 ^c)
HEB	AN	1.2×10^{10}		0.33 (0.397 ^d)
DUR	BN	9.1×10^9	0.019 ^b	0.22
TIPB	BN	5.2×10^9		0.69
HMB	BN	1.1×10^{10}	0.0091 ^b	0.072
HEB	BN	8.0×10^9		0.34
DUR	DCM	8.1×10^9	0.24	0.0043
TIPB	DCM	5.9×10^8		0.23
HMB	DCM	1.3×10^{10}	0.093	0.0048
HEB	DCM	8.0×10^9		0.14
DUR	DCB	2.1×10^9	0.37	0.0014
TIPB	DCB	1.4×10^8		0.026
HMB	DCB	5.0×10^9	0.16	0.0022
HEB	DCB	2.0×10^9		0.083
DUR	THF	8.5×10^9	0.14	0.0034
TIPB	THF	2.2×10^8		0.046
HMB	THF	1.7×10^{10}	0.085	0.011
HEB	THF	9.3×10^9		0.063

^a The internal error in Y_{FRI} (based on repeated experiments) is about 4%. ^b Taken from ref 10a. ^c Value taken from ref 21. ^d Value taken from ref 32.

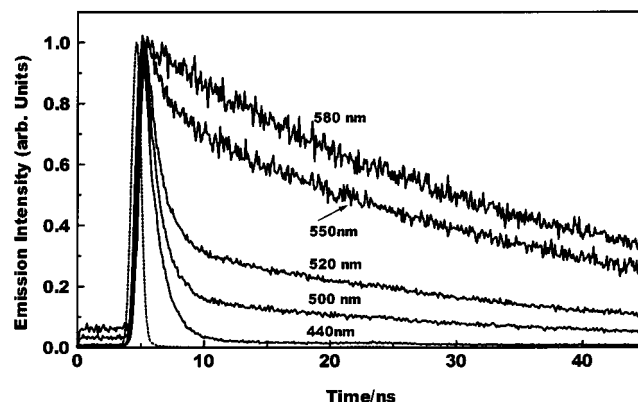


Figure 2. Radiative decay curves for 1.0×10^{-5} M DCA with 0.1 M DUR in DCM at different wavelengths after excitation at 355 nm.

quenching rate constants is less than 50%. This suggests that, when DCA is quenched by HMB rather than DUR, a larger fraction is quenched at long separation distances. If the initial separation distances between geminate RIPs formed following electron transfer have an effect on the FRI yields, changes in FRI yields should be observable.

If the geminate RIPs that result in the formation of free ions have initial distance separation distributions different from those that recombine to the ground state by return electron transfer, there might also be some difference in the dynamics of FRI formation and electron transfer recombination. For the systems considered in the present study, the fluorescence quantum yields are very small. Therefore, the contribution of radiative recombination to the electron transfer recombination rates is negligible. The decay of the exciplex can actually be used to determine the electron transfer recombination rate. The recombination process can be traced by single photon counting and free ion formation can be observed directly by transient photocurrent experiments. Time-resolved emission experiments at different wavelengths on electron-transfer quenching of excited DCA by 0.1 M DUR in DCM indicate the presence of two components (Figure 2). The fast component makes a larger contribution when the emission is monitored on the high energy side and corresponds to DCA monomer fluorescence. Its lifetime, 0.98

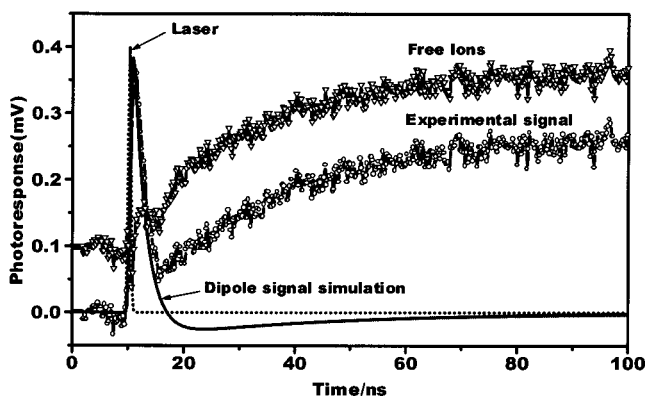


Figure 3. Photoresponse for 1.0×10^{-4} M DCA solution with 0.1 M DUR in DCM after absorption of $20.8 \mu\text{J}$ at 367 nm using a time-resolved transient dc photocurrent technique with 1600 V applied and a 50Ω scope input. The free ion component of the signal has been offset from the experimental curve by an additional 0.1 mV.

ns, is independent of wavelength. At the low energy side (>580 nm), the slow component predominates. It represents emission from the exciplex formed between DCA and DUR after quenching and has a wavelength independent lifetime of 32 ns.

Figure 3 shows a photocurrent trace after quenching of DCA by 0.1 M DUR in DCM. The sharp spike in the photoresponse immediately following excitation is characteristic of a photo-induced dipole. Unlike the pure dipole signal, which returns to zero at long time, the photocurrent rises to a steady positive value. It continues for more than 1 ms and exhibits typical second-order decay kinetics, which is consistent with the expected behavior of free ions. We have reported similar results in previous work for the EDA complex formed between trans-stilbene and fumaronitrile in THF.¹⁹ The lifetime of 32 ns of the DCA–DUR exciplex from time-resolved fluorescence is used to help generate the best fit of the dipole signal from the photocurrent curve, which yields a dipole moment of 17 D for the exciplex.²⁷ After subtracting the dipole signal, the remaining photocurrent represents FRIs and corresponds to a FRI yield of 0.0043. The rise time of this portion of the signal is about 21 ns. We tentatively assign this time constant to the SSRIPs which are dissociating. The free ion yields for electron-transfer quenching by other donors in different solvents are collected in Table 2. Under the experimental condition used, the free ion yield values exhibit no obvious dependence on the applied voltage, whereas the free ion yield values are corrected to zero applied electric field according to the method we used in our previous work.¹⁸

4. Discussion

4.1. Exciplex Fluorescence and Free Ion Quantum Yields.

Gould and Farid determined the efficiencies with which exciplexes or excited charge-transfer (CT) complexes are formed in bimolecular electron-transfer quenching reactions of excited electron acceptors (A^*) by donors (D).¹⁰ They found that, in polar solvents such as AN, the efficiency of exciplex formation is less than unity. This was explained by the formation of SSRIPs from the encounter pair. They also found that the formation efficiencies in moderately polar and nonpolar solvents are essentially unity. The latter case can be understood in two ways. Either the formation of SSRIPs cannot occur in moderately polar and nonpolar solvents because of energy constraints, or the SSRIPs formed immediately after electron-transfer quenching collapse to exciplexes (CRIPs) much faster than RIP separation and long distance return electron transfer reaction.

In this latter case, the recombination rate is not sensitive to the change in initial separation distance, and therefore, measurements of recombination rates cannot provide much information on the initial separation distance distribution following the quenching process. In addition, such measurements do not lend themselves to studies of the effect of the initial separation distance distribution on recombination and free ion formation. In moderately polar solvents such as DCM, THF, and DCB, CRIPs make large contributions to radiative recombination electron transfer, whereas only the long distance RIPs have a high probability of escaping each other. Here it is of interest to compare the fluorescence and free ion quantum yields of different electron donor and acceptor pairs.

In the recent work of Vauthey et al.,¹⁶ the deuterium isotope effect on the fluorescence lifetime and free ion yield of ion pairs formed by electron-transfer quenching were studied. They concluded that, in the polar solvent of AN, the efficiency of free ion formation is determined by direct competition between electron-transfer recombination and dissociation into free ions from a single species CRIP. They believed that LRIPs formed upon quenching do not play a significant role in the charge separation process.

Ion pairs created upon quenching have several possible fates. They may recombine by reverse electron transfer, separate to form FRI, or undergo intersystem crossing. If one assumes no intersystem crossing, the simplest model for these systems involves direct competition between the recombination and separation processes. The recombination rate depends on both the radiative and nonradiative rate constants. The calculation of the nonradiative rate constant involves the product of the square of electronic coupling element, H_{ab}^2 , and a Franck–Condon term, $\text{FC}(\Delta G_{-ET})$:²⁸

$$k_{-ET} = \frac{4\pi^2}{h} H_{ab}^2 \text{FC}(\Delta G_{-ET}) \quad (1)$$

$$H_{ab}^2 = H_{ab}^{\circ 2} \exp[-\beta(r - r_0)] \quad (2)$$

$$\text{FC}(\Delta G_{-ET}) = (4\pi\lambda_s k_B T)^{-1/2} \exp\left(-\frac{(\lambda_v + \lambda_s + \Delta G_{-ET})^2}{4\lambda_s k_B T}\right) \quad (3)$$

In eq 1, h is Planck's constant. The electronic coupling element, H_{ab} , is assumed to decrease exponentially with increasing separation distance r (eq 2), and H_{ab}° is the value of H_{ab} at contact separation distance r_0 . The β factor measures the decrease in electronic coupling with donor/acceptor separation distance. The Franck–Condon term is a function of the free energy change (ΔG_{-ET}) as well as of the solvent (λ_s) and intramolecular (λ_v) reorganization energies. In eq 3, k_B is Boltzmann's constant.

The rate constant for radiative electron transfer k_f is given by²⁹

$$k_f = \frac{64\pi^4}{3h^3 c^3} n^3 \nu_{av} H_{ab}^2 \Delta\mu^2 \quad (4)$$

$$\nu_{av} = \frac{\int I_f \nu d\nu}{\int \frac{I_f}{\nu} d\nu} \quad (5)$$

$$h\nu_{av} = -\Delta G_{-ET} - \lambda_v - \lambda_s \quad (6)$$

where n is the solvent refractive index, ν_{av} is the average emission frequency of CRIPs, c is the speed of light, I_f is the emission rate constant at frequency ν , and $\Delta\mu$ is the magnitude of the difference in static dipole moment of the neutral (DA) and ion pair states (D^+A^-). For CRIPs of DCA–DUR and DCA–HMB in polar and moderately polar solvents, the ion pair states are very similar with more than 85% charge transfer.¹⁰ In this case, we can expect the radiative electron-transfer rate to be proportional to ν_{av} ; in other words, there is little increase in k_f for CRIPs of DCA–DUR compared with those of DCA–HMB.

The escape rate constant k_{ESC} for RIP is often estimated by the Eigen equation:³⁰

$$k_{\text{ESC}} = \frac{3r_c}{r^3_{\text{EXP}}(r/r_c) - 1} D \quad (7)$$

where D is the sum of the ion diffusion constants and r_c is the Onsager radius, $r_c = e^2/(4\pi\epsilon_s\epsilon_0k_B T)$. We do not expect this equation to provide very accurate predictions of k_{ESC} , despite its prevalence in the literature. However, it does prove useful in examining the various trends in our data. Note that k_{ESC} depends both on r , the distance of separation between donor and acceptor, and r_c , the Onsager radius.

If direct competition between radiative electron transfer, nonradiative electron transfer, and the separation process from the CRIP are assumed and no intersystem crossing occurs, quantum yields for radiative return electron transfer and free ion formation can be estimated as

$$\Phi_f = \frac{k_f}{k_{-\text{ET}} + k_f + k_{\text{ESC}}} \quad (8)$$

$$Y_{\text{FRI}} = \frac{k_{\text{ESC}}}{k_{-\text{ET}} + k_f + k_{\text{ESC}}} \quad (9)$$

In moderately polar solvents, both fluorescence and free ion quantum yields, Φ_f and Y_{FRI} , respectively, are far less than 1, and thus, both the rate constant of radiative electron transfer (k_f) and that of escape (k_{ESC}) are significantly smaller than the rate constant of nonradiative electron transfer ($k_{-\text{ET}}$). Therefore, eqs 8 and 9 can be written as

$$\Phi_f = \frac{k_f}{k_{-\text{ET}}} \quad (10)$$

$$Y_{\text{FRI}} = \frac{k_{\text{ESC}}}{k_{-\text{ET}}} \quad (11)$$

As shown in eqs 1, 4, and 7, only k_f , the rate constant for exciplex fluorescence, and $k_{-\text{ET}}$, the nonradiative electron-transfer rate constant, are functions of driving force, $\Delta G_{-\text{ET}}$. Of these two rate constants, $k_{-\text{ET}}$ should be the most strongly dependent on driving force. For CRIPs of DCA–DUR and DCA–HMB, the separation distances and the electronic coupling elements are very similar. We thus expect the relative differences in radiative and escape rate constants for DCA–DUR and DCA–HMB to be very small, and both Φ_f and Y_{FRI} should show a similar dependence on recombination rates. In other words, if we observe an increase/decrease in fluorescence quantum yield from DCA–DUR compared to DCA–HMB in a given solvent, we should observe a similar change in free ion yield. In addition, the recombination rates for the present systems are located in the Marcus inverted region, which means that, at

the same ion pair separation distances, the recombination rate for DCA–DUR is lower than that of DCA–HMB. This will, in turn, cause a larger Φ_f and Y_{FRI} . From Table 2, it can be seen that this is roughly true when AN and BN are used as solvents, where both fluorescence quantum yields and free ion yields for DCA–DUR are about two times that of DCA–HMB. In these polar solvents, the initial separation distance distribution is not expected to be important for the subsequent recombination and escape processes, because there is direct competition between recombination and separation.

The case is much different in moderately polar solvents. In DCB, DCM, and THF, the fluorescence quantum yields for DCA–DUR are always three to four times higher than for DCA–HMB, but no similar trend can be seen in the free ion yields. In DCM, free ion yields are almost the same for both systems, and in DCB and THF, free ions yields for DCA–HMB are larger than those for DCA–DUR. This indicates that recombination rate is not the only factor controlling free ion yields and suggests that another factor, the initial separation distribution, should also be considered in the free ion formation process.

Comparing the recombination rate obtained from time-resolved fluorescence of the exciplex (Figure 2) with that from free ion formation from photocurrent experiments in DCM (Figure 3), it is found that there exists a significant difference between the two. The free ion formation process is faster than the recombination process. Similar results have been reported by Hirata et al.³¹ and in our previous work,¹⁸ but Hirata et al. do not see the dipole signal evident in Figure 3. Moreover, they make no clear interpretation of the different kinetics seen in recombination and free ion formation. It is clear that the ion pairs that recombine to the original ground state and those that separate into free ions have different histories and that there is no direct competition between recombination and separation.

In recent work, we found that for EDA complexes formed between tetracyanoethylene and alkylbenzenes in DCM the radical ion pairs formed by excitation of long-distance random pairs make the predominant contribution to the FRI yield.¹⁹ For the present system, the RIPs are not formed by direct EDA excitation but by quenching, which can take place at larger separation distances. The difference in recombination and free ion formation rates can be understood from the following model. Free ions are mainly formed from initial radical ion pairs separated by long distances. Thus, the free ion yield results from the separation processes involving only long distance pairs. Short-distance ion pairs, which are formed by direct quenching and from collapsed long distance pairs, will slowly recombine to the ground state and make very limited contribution to the free ion yield. In nonpolar and moderately polar solvents, the initial separation distance distribution has a more significant impact on free ion formation than does the recombination rate. For long distance pairs, the main processes that might compete with separation are collapse under the Coulombic field to the CRIP or long distance recombination via electron transfer.

DCA is a weak acceptor; the electron-transfer quenching of excited DCA by the donors used in the present study exhibits Marcus “normal” region characteristics.^{32b} In this region, a stronger donor will result in a larger quenching rate constant and a shift of the quenching separation distribution to longer distances.³³ This can be confirmed by comparing the effect of steric bulk on the electron-transfer quenching rate constant. From DUR to TIPB, the quenching rate constants decrease by a factor of about 2 in polar solvents, whereas in less polar solvents, they decrease by a factor of more than 10. Table 2 indicates that

most of the quenching for DUR takes place at very short distances, so it is very sensitive to the change in contact separation distance.

From HMB to HEB, the change in the quenching rate constant is less than 2-fold in most cases. This implies that long distance quenching is very important for both HMB and HEB. In less polar solvents, only RIPs with long separation distances have a large probability of separating into FRIs. Under these circumstances, it can be expected that RIPs involving DCA and HMB will give a higher free ion yield than those involving DCA and DUR. However, because HMB is a stronger donor, the recombination process exhibits Marcus “inverted” behavior. The driving force for the recombination of RIPs formed between DCA and weaker donors is larger than that between DCA and stronger donors. Thus, it can be expected that the recombination rate constant for the former is smaller than that for the latter pairs. Using a stronger donor shifts the separation distribution of quenching to longer distances, which favors the formation of free ions. Strong donors, however, also increase the recombination rate, which is an unfavorable factor for free ion formation.

As we will discuss later, in polar solvents, where the separation rate exhibits a very weak dependence on the separation distance, the free ion yield is determined by the recombination rate. With DCA in AN and BN, free ion yields from geminate ion pairs formed with DUR are about 3 times higher than those formed with the stronger donor HMB (see Table 2). However, in moderately polar solvents such as DCM and DCB, it is difficult for contact and short distance ion pairs to form free ions because of the strong Coulombic attractions. Only ion pairs separated by long distances have a significant probability of escape. Thus for free ion formation in DCM and DCB, the distribution of initial separation distances for the ion pairs and the rates of recombination are both of significant importance in free ion formation. The free ion yields for DCA–DUR and DCA–HMB are almost the same in DCB and DCM. In THF which is even less polar, the initial separation distance distribution will become even more important, and as expected, DCA–HMB has a FRI yield three times higher than that for DCA–DUR.

4.2. Steric Effects on Free Ion Yields. Free ion yields are controlled by the competition between ion pair separation and recombination in the initially formed radical ion pairs. Steric bulk of the donor increases the minimum separation distance between the acceptor and donor and, thus, influences both the recombination and separation rates.³² Separation requires diffusion of the radical ions against the Coulomb field. Recombination can occur at any point during the diffusion process via electron transfer, although its probability decreases with separation distance. It is unreasonable to consider separation as a one step process or to expect that recombination occurs at a single fixed separation distance. In addition, the distribution of initial separation distances for the radical ion pairs that form free ions is different from the distribution for ions that recombine. Therefore, the rise time of the free ion component is different from the decay time because of recombination as observed in Figure 3. This effect is expected to be largest in nonpolar solvents.

In polar solvents, the distribution of initial separation distances is similar to the distribution in nonpolar solvents, but ions close to contact have a higher probability of forming free ions because of weaker Coulombic forces of attraction and a much shorter Onsager radius, i.e., a much shorter distance required for free ion formation. Because there are many more short distance pairs

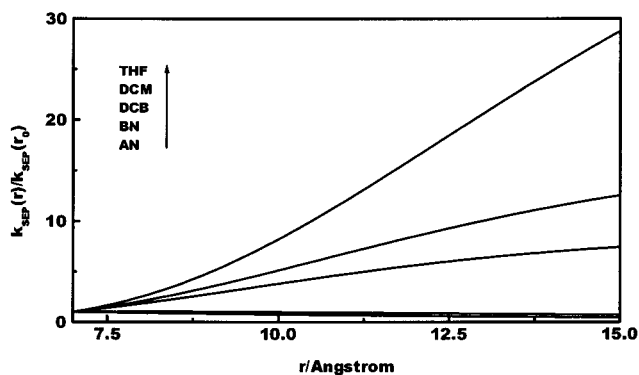


Figure 4. Relative separation rates from eq 12 as a function of separation distances in different solvents. A distance of 3.5 Å was used for the contact distance, r_0 .

created initially and these pairs are more likely to escape than in nonpolar solvents, the significance of the long distance pairs is reduced. Thus, in polar solvents, steric effects change the recombination rate but should not greatly alter the rate of separation. This has been assumed for such systems in polar solvents in the literature. For instance, Gould and Farid studied steric effects on recombination rates by measuring the free ion yields of radical ion pairs formed by the electron-transfer quenching of DCA by sterically hindered alkylbenzenes in AN.^{32b} They assumed the same rate of separation for all of the systems used and calculated the rate constants for recombination of the various donor and acceptor pairs assuming direct competition between recombination and separation. They maintained that the main effect of steric hindrance was to decrease the magnitude of the electronic coupling element for electron transfer, which in turn decreases the electron-transfer recombination rate and, thus, increases the free ion yield.

In less polar solvents, the steric effect on separation rates needs to be considered more carefully to achieve an understanding of the roles of the different factors that control the efficiency of free ion formation. If the separation rate constant at contact distance r_0 for a given solvent is $k_{\text{SEP}}(r_0)$, the relative separation rate for radical ion pairs at different separation r can be roughly estimated from eq 7 to be

$$\frac{k_{\text{SEP}}(r)}{k_{\text{SEP}}(r_0)} = \frac{r_0^3 [\exp(r_c/r_0) - 1]}{r^3 [\exp(r_c/r) - 1]} \quad (12)$$

Figure 4 exhibits the changes of such relative separation rates with separation distances in different solvents. A contact separation distance r_0 of 7 Å was used in the calculation. In the polar solvents AN and BN, the separation rate constants exhibit very weak dependence on separation distances. In these cases, the main factors that determine the free ion yields are the electron-transfer recombination rates. In moderate polarity solvents DCB, DCM, and THF, Figure 4 indicates that the relative separation rate exhibits a strong dependence on separation distance. Compared with sterically unhindered donors DUR and HMB, the sterically hindered donors (TIPB and HEB) will increase the separation distance by 1–1.3 Å. From Figure 4, it can be roughly estimated that such an increase in separation distance will increase the separation rate constant by a factor of 2–2.5. If electron-transfer recombination always takes place at contact separation distance and if there is direct competition between recombination and separation, the steric effect on free ion yields can be estimated from recombination and separation rates.

Gould and Farid found that in the polar solvent acetonitrile the steric effect could result in a 2–4 fold increase in free ion yields.^{32b} As mentioned previously, although the steric effect on separation rate can be ignored in polar solvents, the increase in donor bulk and thus separation distance does affect the recombination rate. As indicated in eqs 1–3, the recombination rate constant can be altered by changes in driving force, reorganization energy, or the electronic coupling element. Gould and Farid suggest that the main contribution to the alteration of the recombination rate comes from the steric effect on the electronic coupling element.

Recently, we studied the steric effect on the recombination and fluorescence quantum yields of exciplexes formed between tetracyanobenzene and the alkylbenzene donors used in the present work.³⁴ We found that the steric effect decreases the recombination rate by a factor of 1.5–2 in nonpolar solvents such as toluene and benzene. The main contribution for such a change comes from the steric effect on the electronic coupling element. Changes in driving force and reorganization energy effect only small changes in recombination rates. On the basis of these results, we can expect that, in the less polar solvents used in this study, the steric effect will increase the separation rate by a factor of 1.5–2 and decrease the recombination rate by a factor of 2–4. If the steric effects on both the recombination rate and the separation rate are combined, it is reasonable to expect the increase in free ion yield to be about 3–10 times. From Table 2, it can be seen that the free ion yields involving bulky donors in moderately polar solvents can be more than 40 times larger than those of unhindered donors! It is difficult to understand such a result from the simple mechanism in which there is a direct competition between separation and recombination at contact separation distance.

From the steric effect on quenching rate constants, we have concluded above that most of the quenching for the DCA-DUR system takes place at very short separation distances, whereas for the DCA-HMB system, long distance quenching is also effective. Comparing the free ion yield increase induced by additional steric hindrance, we find that the accompanying increase in free ion yield from HMB to HEB is always less than that from DUR to TIPB in moderately polar solvents. This is consistent with a quenching separation distance distribution and provides further evidence that the initial separation distance distribution is a very important factor in FRI formation.

4.3. Mechanism of FRI Formation. Even in polar solvents, RIPs formed by direct excitation of EDA complexes and quenching of excited free acceptors by electron donors lead to different quantum yields for FRI formation.^{13a} This indicates that the initial distribution of separation distances is an important factor that controls free ion yields. By comparing the recombination rate obtained from time-resolved fluorescence (32 ns) and the rise time of the photocurrent obtained from transient photoconductivity (21 ns) in DCM, it is clear that recombination and free ion formation obey different kinetics. RIPs resulting in free ion formation have different histories than those that recombine.

The importance of the initial distance distribution of ions is reflected in the Onsager equation,³⁵ which is often used to estimate the FRI yield, $Y_{\text{FRI}}^{\text{O}}$:

$$Y_{\text{FRI}}^{\text{O}} = \exp(-r_c/R_0) \quad (13)$$

Here, R_0 represents the initial separation distance between donor cation and acceptor anion. This equation assumes point charges in a dielectric continuum with a perfect sink at $r = 0$. Further

explanation of the conditions for this equation can be found in the literature.^{35,36}

For the systems under discussion here, the collapse or recombination of RIPs takes place at a large range of separation distances. No equilibrium distribution exists among the RIPs at different separation distances during the decay process. The Onsager radii for DCM and THF are 63 and 74 Å, respectively. For CRIPs with an initial separation distance of 3.5 Å in these moderately polar solvents, FRI yields estimated using the Onsager equation are 1.6×10^{-9} and 6.5×10^{-11} , respectively, much lower than experimental results. Even for LRIPs with a separation distance of 7.0 Å, the predicted FRI yields are 1.24×10^{-4} and 2.5×10^{-5} . The free ion yield values for both DCA-DUR and DCA-HMB are more than 5×10^{-3} in DCM and more than 4×10^{-4} in THF. An R_0 value of at least 12 Å would be required in the Onsager equation to fit these yields.

The Onsager equation may not appropriately model the exciplex systems considered here for additional reasons. In the solvents used in the present study, only CRIPs can give exciplex emission. No exciplex emission from long distance separated radical ion pairs can be observed. Therefore, the decay rate obtained from time-resolved fluorescence experiments is directly related to the total radiative and nonradiative recombination processes of CRIPs. Additionally, the rise time of the photocurrent (Figure 3) is 21 ns for DCA-DUR, which differs from the 32 ns decay time of CRIPs obtained from time-resolved fluorescence. This means that the radical ion pairs forming FRIs are different in nature from the CRIPs and have a lifetime of roughly 21 ns before direct recombination or collapse to CRIPs. This lifetime is especially surprising when one considers that two opposite charged ions separated by 10 Å in a dielectric continuum with $\epsilon = 8.93$ (DCM) should recombine in roughly 20 ps.³⁷ However, this calculation ignores both the structure of the solvent and solvation which surely become important as the ions approach each other. The observed photocurrent rise time (21 ns) indicates a much longer lifetime (by roughly 3 orders of magnitude!) for these species and suggests the existence of a significant energy barrier between the SSRIP and CRIP. If there is not a fast equilibrium between CRIPs and SSRIPs, the rise time of the photocurrent should represent the decay of the LRIP. In most cases, the FRI yield is small; therefore, the decay of LRIPs is dominated by either the collapse of SSRIP to CRIP or the long distance recombination of the SSRIP. Because LRIPs are responsible for the FRI yield, the case in which an imperfect sink exists at a distance representative of the SSRIP should be considered.

With this in mind, the Collins and Kimball (partially reflective) boundary condition³⁸ is more appropriate than is the perfect sink boundary condition used by Onsager. This boundary condition is included in the theory of Hong and Noolandi,³⁹ which states that the FRI yield for RIPs with Coulombic interactions can be estimated by^{36,40,41}

$$Y_{\text{FRI}}^{\text{HN}} = \frac{\exp(-r_c/R_0) + (z-1)\exp(-r_c/r_m)}{1 + (z-1)\exp(-r_c/r_m)} \quad (14)$$

where r_m is the critical reaction radius, z is a dimensionless constant defined as $z = Dr_c/\kappa r_m^2$, and κ is the surface recombination or decay rate constant. For RIPs with a lifetime τ , κ may be taken to be r_m/τ and D is the sum of the ion diffusion constants.

Figure 5 shows plots of calculated FRI yields against the initial separation distance R_0 at different critical reaction radii r_m in DCM. It can be seen that the free ion yield is very sensitive

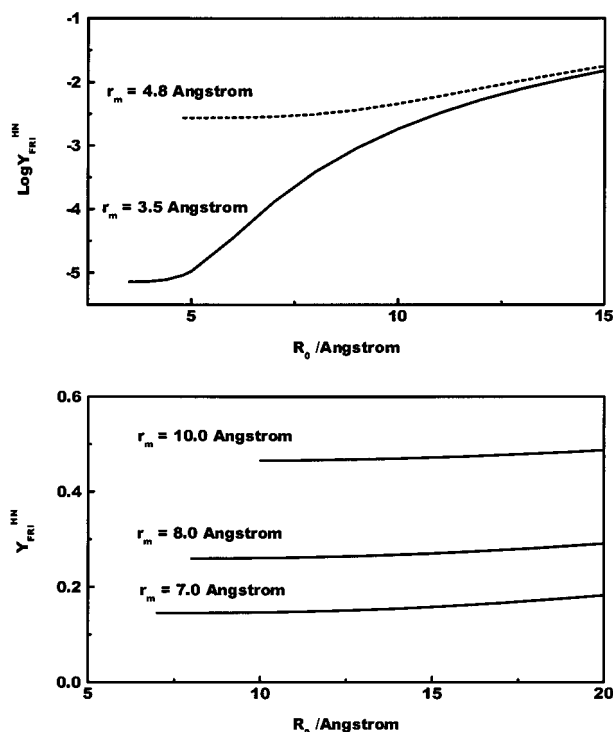


Figure 5. Plots of FRI yields calculated from eq 14 vs the initial separation distance R_0 at different critical reaction radii r_m in DCM. Parameters used in these calculations are $r_c = 63 \text{ \AA}$, $D = 3.6 \times 10^{-5} \text{ cm}^2 \text{ s}^{-1}$, and $\tau = 21 \text{ ns}$ (obtained from the observed photocurrent rise time for DCA–DUR).

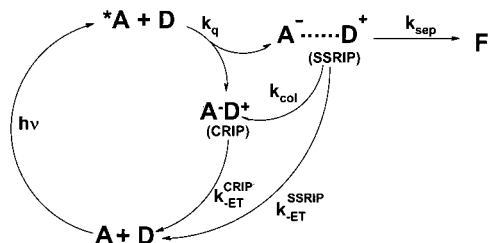
to a change of r_m . For the sake of comparison, with an r_m and R_0 value of 3.5 \AA , which corresponds to the typical separation in a CRIP, the calculated free ion yields are far less than the experimental result of 4.3×10^{-3} as seen in the figure. Even if the RIPs are formed with an initial separation distance of 7.0 \AA , which corresponds to the separation distance for SSRIPs, with an r_m value of 3.5 \AA , the calculated FRI yield is only about 1×10^{-4} , roughly 2 orders of magnitude less than the experimental results. For DCA–DUR in DCM, the separation distance for the SSRIPs is about 7 \AA , and it is reasonable to assume $r_m = 7 \text{ \AA}$ for the free ion yield calculation if a barrier exists between the CRIP and SSRIP. From Figure 5, it can be seen that the free ion yields increase from 0.15 to 0.18 when the initial separation distance increases from 7.0 to 20.0 \AA . This suggests that for $r_m = 7 \text{ \AA}$ the free ion yield is not sensitive to the variation in the initial separation distance. This calculated value for the FRI yield is much greater than the experimental result.

The electron-transfer quenching rate constant for DUR is about 15 times larger than that for TIPB in DCM; that is, more than 94% of the quenching in DCA–DUR will result in the formation of short distance separated contact radical ion pairs which make almost no contribution to free ion formation. Less than 6% of the total DUR quenching will result in the formation of long distance separated ion pairs. In this case, the free ion yield can be calculated by eq 15:

$$Y_{\text{FRI}}^{\text{HN}} = \delta \left[\frac{\exp(-r_c/R_0) + (z-1) \exp(-r_c/r_m)}{1 + (z-1) \exp(-r_c/r_m)} \right] \quad (15)$$

where δ is the ratio of long distance quenching in the total electron-transfer quenching. Using $R_0 = 7.0 \text{ \AA}$ and $\delta = 0.06$, the calculated free ion yield is 9.0×10^{-3} , which fits the experimental result of 4.3×10^{-3} reasonably well. For DCA–

SCHEME 2: Mechanism for Free Ion Formation from the Geminate Radical Ion Pairs Produced by Electron Transfer Quenching



TIPB, the separation distance for SSRIPs with one layer of DCM solvent is about 8.0 \AA . From Figure 5, we find that, when $r_m = 8.0 \text{ \AA}$ and $\delta = 1.0$, the calculated free ion yield changes from 0.25 to 0.28 as the initial separation distances change from 8.0 to 20.0 \AA . This value also fits the experimental result quite well. However, if a contact separation distance of 4.8 \AA is used for r_m , the calculated free ion yield is more than 100 times lower than the experimental. This suggests that most of the quenching for DCA–TIPB will result in the formation of SSRIPs. For other systems and in other solvents, similar fits can be obtained.

On the basis of both the above discussion and the results presented in previous sections, we propose the mechanism for recombination and free ion formation depicted in Scheme 2. In moderately polar solvents, the electron-transfer quenching of excited acceptor DCA by electron donors such as DUR and HMB results in the direct formation of two different kinds of ion pairs, the CIPs and the long distance SSRIPs. There is no equilibrium between the two species during decay processes. The main decay processes for contact ion pairs are radiative and nonradiative recombination. The number of CRIPs which form free ions is insignificant. SSRIPs can stay at long separation distances for quite a long time. For instance, for DCA–DUR in DCM, the lifetime for the solvent separated ion pair could be as long as 21 ns before direct recombination or collapse to contact ion pairs. This significantly increases the probability that the ion pairs will separate into free ions and indicates that there is a high activation energy required for the transformation between SSRIPs and CRIPs. It is unclear whether SSRIPs form CRIPs before recombination or if they recombine directly to the ground state and thus bypass CRIP formation.

It should be mentioned that SSRIPs are long distance separated radical ion pairs. Their formation and decay should proceed from a broad separation distance distribution. However, there are probably no high potential barriers between these SSRIPs, so there always exists an equilibrium among them during recombination and separation processes. Actually, the 21 ns rise time portion of the signal should be understood as the average decay time of the SSRIPs with different separations.

5. Conclusions

We report FRI and fluorescence quantum yields following the electron-transfer quenching of photoexcited DCA by a group of aromatic electron donors in a variety of solvents. The effects of steric bulk and solvent polarity were analyzed to gain insight into the kinetics of these systems and, in particular, into the role of initial separation distance distribution following quenching. In polar solvents, the increased initial separation distance caused by steric bulk of the donor results in FRI yields which correlate well with trends in electron transfer recombination rates. In moderately polar solvents, FRI yields of the acceptor and donor pairs involving bulkier donors have much higher FRI yields than would be expected from recombination rate trends

alone, and thus, the initial separation distance distribution plays a much more significant role in the separation process. In addition, comparison of the photocurrent rise time and the exciplex lifetime from fluorescence in DCM confirms that the pairs that separate and those that recombine have different histories and suggests the existence of an energy barrier between the SSRIP and CRIP. The results were fit using theory by Hong and Noolandi and support the mechanism proposed in this work.

Acknowledgment. The authors acknowledge support of this work from the Division of Chemical Sciences, Office of Basic Energy Sciences, U.S. Department of Energy, under Grant DE-FG02-86ER13592.

References and Notes

- (1) (a) Miller, J. R. *Science* **1975**, *189*, 221. (b) Beitz, J. V.; Miller, J. R. *J. Chem. Phys.* **1979**, *71*, 4579. (c) Miller, J. R.; Hartman, K. W.; Abrash, S. *J. Am. Chem. Soc.* **1982**, *104*, 4296
- (2) Guarr, T.; McGuire, M.; Strauch, S.; McLendon, G. *J. Am. Chem. Soc.* **1983**, *105*, 616.
- (3) (a) Miller, J. R.; Calcaterra, L. T.; Closs, G. L. *J. Am. Chem. Soc.* **1984**, *106*, 3047. (b) Closs, G. L.; Miller, J. R. *Science* **1988**, *240*, 440.
- (4) Wasielewski, M. R.; Niemczyk, M. P.; Svec, W. A.; Pewitt, E. B. *J. Am. Chem. Soc.* **1985**, *107*, 1080.
- (5) Isied, S. S.; Vassilian, A.; Wishart, J. F.; Creutz, C.; Schwarz, H. A.; Sutin, N. *J. Am. Chem. Soc.* **1988**, *110*, 635.
- (6) (a) Oevering, H.; Paddon-Row, M. N.; Heppener, M.; Oliver, A. M.; Cotsaris, E.; Verhoeven, J. W.; Hush, N. S. *J. Am. Chem. Soc.* **1987**, *109*, 3258. (b) Penfield, K. W.; Miller, J. R.; Paddon-Row, M. N.; Cotsaris, E.; Oliver, A. M.; Hush, N. S. *J. Am. Chem. Soc.* **1987**, *109*, 5061. (c) Schuddeboom, W.; Scherer, T.; Warman, J. M.; Verhoeven, J. W. *J. Phys. Chem.* **1993**, *97*, 13092. (d) Rost, M. R.; Lawson, J. M.; Paddon-Row, M. N.; Verhoeven, J. W. *Chem. Phys. Lett.* **1994**, *230*, 536.
- (7) (a) Cave, R. J.; Newton, M. D.; Kumar, K.; Zimmt, M. B. *J. Phys. Chem.* **1995**, *99*, 17501. (b) Kumar, K.; Lin, Z.; Waldeck, D. H.; Zimmt, M. B. *J. Am. Chem. Soc.* **1996**, *118*, 243.
- (8) (a) Hung, S.-C.; Macpherson, A. N.; Lin, S.; Liddell, P. A.; Seely, G. R.; Moore, A. L.; Moor, T. A.; Gust, D. *J. Am. Chem. Soc.* **1995**, *117*, 1657. (b) Macpherson, A. N.; Liddell, P. A.; Lin, S.; Noss, L.; Seely, G. R.; DeGraziano, J. M.; Moore, A. L.; Moor, T. A.; Gust, D. *J. Am. Chem. Soc.* **1995**, *117*, 7202.
- (9) (a) Knibbe, H.; Röllig, K.; Schäfer, F. P.; Weller, A. *J. Chem. Phys.* **1967**, *47*, 1184. (b) Knibbe, H.; Rehm, D.; Weller, A. *Ber. Bunsen-Ges. Phys. Chem.* **1968**, *72*, 257. (c) Beens, H.; Weller, A. In *Organic Molecular Photochemistry*; Birks, J. B., Ed.; Wiley: New York, 1975; Vol. 2, Chapter 4.
- (10) (a) Gould, I. R.; Young, R. H.; Mueller, L. J.; Farid, S. *J. Am. Chem. Soc.* **1994**, *116*, 8176. (b) Gould, I. R.; Young, R. H.; Mueller, L. J.; Albrecht, A. C.; Farid, S. *J. Am. Chem. Soc.* **1994**, *116*, 8188.
- (11) (a) Asahi, T.; Mataga, N. *J. Phys. Chem.* **1989**, *93*, 6575. (b) Mataga, N. *J. Phys. Chem.* **1991**, *95*, 1956. (c) Asahi, T.; Ohkohchi, M.; Mataga, N. *J. Phys. Chem.* **1993**, *97*, 13132. (d) Mataga, N.; Miyasaka, H. *Prog. React. Kinet.* **1994**, *19*, 317.
- (12) (a) Jones, G., II.; Chiang, S.-H.; Becker, W. G.; Welch, J. A. *J. Phys. Chem.* **1982**, *86*, 2805. (b) Jones, G., II. In *Photoinduced Electron Transfer, Part A, Conceptual Basis*; Fox, M. A., Chanon, M., Eds.; Elsevier: New York, 1988; p 245.
- (13) (a) Gould, I. R.; Young, R. H.; Moody, R. E.; Farid, S. *J. Phys. Chem.* **1991**, *95*, 2068. (b) Gould, I. R.; Young, R. H.; Farid, S. In *Photochemical Processes in Organized Molecular Systems*; Honda, K., Ed.; Elsevier: New York, 1991; p 19.
- (14) (a) Mataga, N.; Kanda, Y.; Okada, T. *J. Phys. Chem.* **1986**, *90*, 3880. (b) Mataga, N.; Asahi, T.; Kanda, Y.; Okada, T.; Kakitani, T. *Chem. Phys.* **1988**, *127*, 249. (c) Both LRIP and SSRIP represent radical ion pairs (RIPs) which are not at contact. The designation of LRIP is more general than that of SSRIP and refers to any RIP which is neither at contact nor free. An SSRIP is sometimes depicted as the donor cation and acceptor anion separated by a single solvent molecule.
- (15) O'Driscoll, E.; Simon, J. D.; Peters, K. S. *J. Am. Chem. Soc.* **1990**, *112*, 7091.
- (16) Muller, P.-A.; Hogemann, C.; Allonas, X.; Jacques, P.; Vauthey, E. *Chem. Phys. Lett.* **2000**, *326*, 321.
- (17) Arnold, B. R.; Noukakis, D.; Farid, S.; Goodman, J. L.; Gould, I. R. *J. Am. Chem. Soc.* **1995**, *117*, 4399.
- (18) Findley, B. R.; Smirnov, S. N.; Braun, C. L. *J. Phys. Chem. A* **1998**, *102*, 6385.
- (19) Zhou, J.; Findley, B. R.; Teslja, A.; Braun, C. L.; Sutin, N. *J. Phys. Chem. A* **2000**, *104*, 11512.
- (20) Zhou, J.; Findley, B. R.; Braun, C. L.; Sutin, N. *J. Chem. Phys.* **2001**, *114*, 10448.
- (21) Gould, I. R.; Ede, D.; Moser, J. E.; Farid, S. *J. Am. Chem. Soc.* **1990**, *112*, 4290.
- (22) (a) Kikuchi, K.; Takahashi, Y.; Hoshi, M.; Niwa, T.; Katagiri, T.; Miyashi, T. *J. Phys. Chem.* **1991**, *95*, 2378. (b) Inada, T. N.; Miyazawa, C. S.; Kikuchi, K.; Yamauchi, M.; Nagata, T.; Takahashi, Y.; Ikeda, H.; Miyashi, T. *J. Am. Chem. Soc.* **1999**, *121*, 7211.
- (23) (a) Peters, K. S.; Lee, J. *J. Am. Chem. Soc.* **1993**, *115*, 3643. (b) Li, B.; Peters, K. S. *J. Phys. Chem.* **1993**, *97*, 13145.
- (24) Vauthey, E.; Högemann, C.; Allonas, X. *J. Phys. Chem. A* **1998**, *102*, 7362.
- (25) Smirnov, S. N.; Braun, C. L. *Rev. Sci. Instrum.* **1998**, *69*, 2875.
- (26) This distance is estimated from molecular modeling.
- (27) Although a dipole moment of 17 D corresponds with a charge separation of roughly 3.5 Å, we do not expect that this measured dipole moment represents a single structure for the donor cation and acceptor anion pair but rather some sort of average of many pairs at a distribution of separation distances, most of which are at 3.5 Å.
- (28) (a) Brunschwig, B. S.; Ehrenson, E.; Sutin, N. *J. Am. Chem. Soc.* **1984**, *106*, 6858. (b) Sutin, N. In *Electron Transfer in Inorganic, Organic, and Biological Systems*; Bolton, J. R., Mataga, N., McLendon, G., Eds.; Advances in Chemistry Series 228; American Chemical Society: Washington, DC, 1991; p 25.
- (29) (a) Gould, I. R.; Noukakis, D.; Gomez-Jahn, L.; Young, R. H.; Goodman, J. L.; Farid, S. *Chem. Phys.* **1993**, *176*, 439. (b) Gould, I. R.; Noukakis, D.; Goodman, J. L.; Young, R. H.; Farid, S. *J. Am. Chem. Soc.* **1993**, *115*, 3830. (c) Gould, I. R.; Young, R. H.; Mueller, L. J.; Albrecht, A. C.; Farid, S. *J. Am. Chem. Soc.* **1994**, *116*, 3147.
- (30) Eigen, M. *Z. Phys. Chem. N. F.* **1954**, *1*, 176.
- (31) Hirata, Y.; Kanda, Y.; Mataga, N. *J. Phys. Chem.* **1983**, *87*, 1659.
- (32) (a) Jones, G., II.; Chatterjee, S. *J. Phys. Chem.* **1988**, *92*, 6862. (b) Gould, I. R.; Farid, S. *J. Phys. Chem.* **1993**, *97*, 13067.
- (33) Murata, S.; Tachiya, M. *J. Phys. Chem.* **1996**, *100*, 4064.
- (34) Zhou, J.; Braun, C. L. Manuscript in preparation.
- (35) (a) Onsager, L. *J. Chem. Phys.* **1934**, *2*, 599. (b) Onsager, L. *Phys. Rev.* **1938**, *54*, 554.
- (36) Mauzerall, D.; Ballard, S. G. *Annu. Rev. Phys. Chem.* **1982**, *33*, 377.
- (37) This time can be estimated using $\tau = (4\pi\epsilon_0\epsilon r_0^3)/3\mu e$, where r_0 is the initial distance between the ions, μ is the sum of the ion mobilities, and e is the charge on the electron.
- (38) Collins, F. C.; Kimball, G. E. *J. Colloid Sci.* **1949**, *4*, 425.
- (39) (a) Hong, K. M.; Noolandi, J. *J. Chem. Phys.* **1978**, *68*, 5163. (b) Noolandi, J.; Hong, K. M. *J. Chem. Phys.* **1979**, *70*, 3230.
- (40) (a) Berlin, Y. A.; Cordier, P.; Delaire, J. A. *J. Chem. Phys.* **1980**, *73*, 4619. (b) Sano, H.; Tachiya, M. *J. Chem. Phys.* **1979**, *71*, 1276.
- (41) Braun, C. L. *J. Chem. Phys.* **1984**, *80*, 4157.